ULTRASONIC BIOPHYSICS

LEON A. FRIZZELL, *Bioacoustics Research Laboratory, Department of Electrical and Computer Engineering, University of Illinois, Urbana, Illinois, U.S.A.*

INTRODUCTION

The field of ultrasonic biophysics is very broad, encompassing a large range of frequencies and many different biological systems. The modern use of ultrasound started several decades ago in the form of sonar for military applications. Since then it has developed to the point where it is used very extensively in industry, bioengineering, and medicine. Its original applications in medicine were for therapy, where the energy absorbed from ultrasound waves was used to heat a variety of tissues and structures lying below the body surface. Ultrasound could penetrate and deposit heat within these tissues, whereas insufficient heat could be conducted from surface sources. Improved instrumentation and techniques available after World War II led to the development of ultrasound systems for medical imaging. Over the past 35 years ultrasound has developed into an indispensable clinical diagnostic tool. Currently, ultrasound is used to image most parts of the body, and more than half of all pregnant women in the United States are examined with ultrasound. This widespread utilization has resulted from ultrasound's proven clinical utility for imaging soft tissues compared to more expensive imaging techniques. The development of ultrasound, particularly for fetal examinations, has also been fostered by its safety record; no case of an adverse biological effect induced by diagnostic ultrasound has ever been reported in humans (AIUM, 1993).

Ultrasound has been used for many years to characterize biological materials. This results in large part from a desire to understand better the interaction of ultrasound with biological tissues so that clinical ultrasonic systems might be made more efficacious. However, ultrasound has also found application to the determination of rate constants in chemical reactions and in recent years has been used, via ultrasonic cavitation, to enhance desired chemical reactions that normally occur very slowly or not at all. The latter application has spawned the area of sonochemistry (Suslick, 1988), which has the potential for significantly increasing industrial production of many important chemical products, but which is beyond the scope of this article and will not be discussed further.

3-527-29475-9/98/$5.00 + .50

Section 1 discusses some of the basic principles underlying the use of ultrasound in medical imaging, therapy, and other applications. This is followed by discussions of the acoustical characteristics of biological media and the techniques for measuring them. The article ends with a brief discussion of recent developments in medical imaging and therapy.

1. BASIC PRINCIPLES

Unlike electromagnetic waves, acoustic waves require a medium for propagation. The acoustic wave phenomenon causes displacement of particles (consisting of many molecules), which results in pressure and density changes within the medium. For a traveling sinusoidal wave the variation in acoustic pressure (the difference between the total and ambient pressure) can be represented by the form

$$p = Pe^{-Ax}\cos(\omega t - kx) \tag{1}$$

for a wave propagating in the positive x direction, where p is the acoustic pressure, P is its amplitude, $\omega = 2\pi f$ is the angular frequency where f is the frequency in hertz, $k = \omega/c$ is the propagation constant where c is the propagation speed, A is the attenuation coefficient, and t is the time. The same form applies to the excess density, particle displacement, particle velocity, and particle acceleration. The wave can experience significant attenuation, as represented by the exponential decay of amplitude with distance, during propagation in tissues. This attenuation is due in the most part to absorption—conversion of the energy in the wave to heat—and, to a much lesser degree, scattering of energy in different directions. This loss of energy with propagation is important to both diagnostic and therapeutic applications. The attenuation coefficient increases roughly linearly with frequency, but its value varies greatly among tissues (Goss *et al.*, 1978, 1980; Haney and O'Brien, 1986). It is low for most body fluids, much higher for solid tissues, and very high for bone and lung; see Secs. 2.1 and 2.2 for more detail.

The relation given by Eq. (1) is a linear relation, which applies only to low-amplitude waves. In many of the applications discussed here, the amplitude is sufficiently high that significant nonlinear propagation effects may occur. These effects include harmonic generation, where an initially sinusoidal wave will become distorted as it propagates. The distortion can be viewed as the transfer of energy from the initial, or fundamental, frequency of the wave to higher harmonics. Associated with this is an increase in attenuation of energy because the higher frequencies have a higher attenuation coefficient.

Ultrasound is typically used to image soft body tissues such as liver, but the sound beam often travels through fluids—for example, through amniotic fluid when imaging the fetus. Generally, bone and lung are not imaged with ultrasound, largely because of their very large attenuation. The attenuation processes include absorption, which is the conversion of acoustic energy to heat, and scattering, which is addressed later. The attenuation increases roughly linearly with frequency in the 2–10-MHz range typically used for medical imaging. This range represents a compromise between increased penetration at lower frequencies (due to decreased attenuation) and improved resolution associated with higher frequencies as discussed below. Thus, the lower frequencies are used when greater penetration is required such as for fetal imaging in the obese patient and higher frequencies for lesser penetration such as the examination of peripheral vascular flow.

When an acoustic wave impinges on an interface between two media of different specific acoustic impedance, a portion of the incident energy is reflected. For normal incidence on an infinite plane interface, the pressure reflection coefficient is given by (Kinsler *et al.*, 1982)

$$R = (z_2 - z_1)/(z_2 + z_1), \tag{2}$$

where z_1 and z_2 are the specific acoustic impedances of the incident and transmitting media, respectively. For a plane wave the specific acoustic impedance is equal to the characteristic impedance, which is the product of the density and acoustic speed in the medium. The speed is dependent upon the density and the elastic properties of the medium. Thus at an interface between media exhibiting different densities or elastic properties, e.g., compressibility, some acoustic energy will be reflected. Although the reflec-

tion coefficient at an interface between muscle and bone is large (approximately 0.54), the reflection coefficient between two soft tissues such as liver and muscle is quite small (approximately 0.006). Reflection at oblique incidence obeys Snell's law (Kinsler *et al.*, 1982).

In addition to the specular reflection that occurs at an interface between two media of different specific acoustic impedance as described above (where any curvature along the interface is negligible over distances comparable to a wavelength), energy may also be scattered in all directions by inhomogeneities in the medium. An acoustic image is formed by using this scattered energy as well as specular reflections. The fraction of the incident energy reflected or scattered is very small.

Though it is convenient to consider plane waves of infinite lateral extent, as was done above, real sources generate finite beams of ultrasound. These sources may be unfocused, but for many of the applications discussed here, they are focused. Figure 1 shows the acoustic field from a typical focused source. The source consists of a piezoelectric transducer, which converts electrical to acoustic energy and vice versa. Most transducers for bioengineering and medical applications are made from ceramic materials such as a lead zirconate titanate (PZT) mixture; however, composite materials consisting of a combination of ceramic and other materials are sometimes used as sources, and polyvinylidene difluoride material is used for hydrophone transducers for measuring the ultrasound fields of sources. A circular-aperture focused source may consist of a circular disk with a plano-concave lens mounted in front to produce spherical focusing. Alternatively,

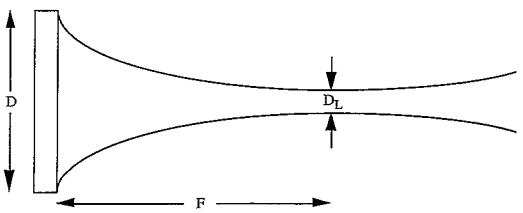

FIG. 1. Cross section of a typical focused circular ultrasound source of aperture diameter D and focal length F showing the focused beam of lateral beam width at the focus D_L.

the transducer itself may be a spherical segment that produces a focused field without a lens. However, increasingly these sources utilize electronic focusing methods. Such a phased-array source consists of many small individual elements, which can be excited with signals having a controlled delay with respect to one another such that the acoustic pressure fields from all elements constructively interfere at the desired focal region. Similarly, in a phased-array receiver, the signals from the different elements are combined after applying delays that result in reinforcement of the signals from a receiving focal region.

The 3-dB lateral beam width D_L of the focused source is directly dependent upon the wavelength and focal length and inversely related to the aperture diameter (diameter of the transducer) D (Kino, 1987):

$$D_L = 1.02F\lambda/D. \tag{3}$$

Because $f\lambda = c$, the higher the frequency, the smaller is λ and D_L. For therapy systems, the energy flux per unit area (intensity) is increased when the source is strongly focused, i.e., D_L is small compared to D. For imaging systems, the smaller D_L, the better the lateral resolution near the focus, though the beam spread is greater with distance from the focus. Thus, for imaging, the strength of the focusing varies among transducers so that the user may choose very good resolution over a short region or somewhat poorer resolution that is maintained over a greater depth. With phased-array transducers, the focal region can be varied dynamically to optimize lateral resolution at all distances.

The discussion above is based on linear propagation. However, in medical imaging and therapy the amplitudes are usually so large that nonlinear propagation occurs. Nonlinear propagation is characterized by increasingly greater distortion of the wave toward the formation of a shock wave as it propagates. Thus, a wave that is initially a sinusoid will develop, in a low-loss medium, into a sawtooth wave over a propagation distance that varies inversely with initial amplitude. This distortion can also be represented in the frequency domain by the transfer of energy into higher-frequency harmonics as the wave propagates. Since energy is transferred to higher frequencies, the attenuation

increases with the nonlinear propagation. In addition to the dependence on amplitude, the nonlinear distortion is dependent on properties of the medium. Specifically, the relation between acoustic pressure and density for liquids is nonlinear and varies with the medium. A parameter that characterizes the degree of nonlinearity in this relation is B/A, the ratio of the quadratic to linear coefficients in the Taylor series expansion of the relation between pressure and density; B/A is called the *nonlinearity parameter*. The larger B/A, the greater is the rate of wave distortion with propagation.

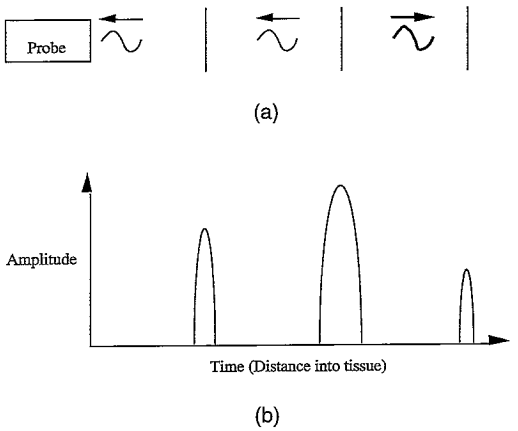

FIG. 2. Illustration of (a) the transmitted pulse (heavy wave) and echoes from reflecting structures and (b) the resulting *A*-mode display.

1.1 Principles of Pulse-Echo Ultrasound

Ultrasound imaging usually employs frequencies in the 2–10-MHz range, though some of the new intracavitary probes use higher frequencies. Images are formed by using a transducer within a probe to generate a short pulse (typically on the order of 1 μs or less in duration) of ultrasound that is propagated through the tissue. A portion of the energy in this pulse is reflected back toward the transducer from specular reflectors and from scatterers in the tissue. These acoustic echoes, with amplitudes much lower than the transmitted pulse, are converted by the transducer to electrical signals that are converted to a (rectified) video signal, amplified by a time-gain-controlled amplifier, and displayed. The time-gain-controlled amplifier increases the gain as a function of time so that later-arriving signals, coming from deeper within the body, are amplified more to compensate for the attenuation. The *A*-mode display is rarely used but simply involves display of the received echoes as amplitude versus time of arrival. The time of arrival is related by the wave speed to the tissue depth from which the echo returns, i.e., $d = ct/2$. This assumes that the speed does not vary with tissue depth, which is a good first-order approximation for soft tissues. Figure 2 provides a very simple representation of this process where the *A*-mode display associated with specular reflection from three different interfaces is illustrated. For clinical imaging the interfaces would not necessarily be perpendicular to the axis of the sound beam, and there would be a continuum of echoes, a continuous received signal, due to energy back-scattered from within the tissues. Since the ultrasound pulse is attenuated exponentially as it propagates, all ultrasonic imaging systems employ a logarithmic variation of amplifier gain with time to compensate the attenuation by the tissue. Thus, echoes from structures reflecting or back-scattering the same fraction of the incident signal will have the same amplitude after passing through the time-gain-controlled amplifier.

A *B*-mode display is typically used for ultrasound imaging. It involves display of the echoes at various brightness or gray levels corresponding to their amplitude. A two-dimensional *B*-mode display involves movement of the transducer (manually or automatically), movement of a mirror to change the direction of the field (automatically), or movement of the ultrasound beam directly (electrically) such that it scans a plane through the body. Figure 3 provides a simplified representation (again, echoes are shown as arising from interfaces only) of the formation of a *B*-mode image. The direction of the beam is monitored so that the received signals along each path are placed in their correct location on the display. Typically, the orientation information and echoes are processed by a digital scan converter for appropriate display of the two-dimensional image on a cathode-ray tube in the standard format used for television picture display. Most *B*-mode systems in use today create an image in 0.1 s or less, so that the image is displayed in real time for viewing of moving

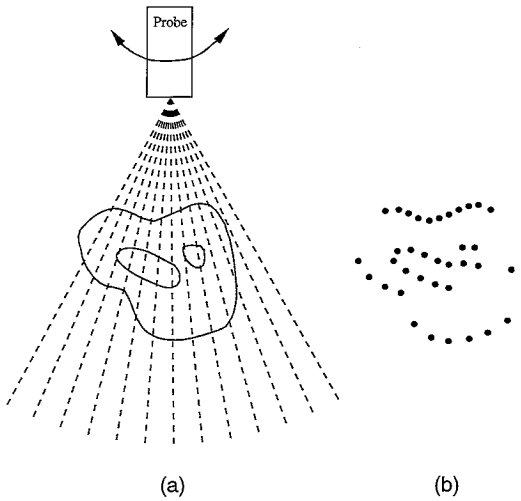

FIG. 3. Illustration of (a) the transmitted pulse paths for a rotating transducer probe and (b) the resulting two-dimensional *B*-mode display of echoes from the interfaces only.

structures, such as structures in the heart or the fetus moving within the womb. This is not possible with the typical magnetic-resonance or computed-tomography system.

Many systems now employ digital processing to enhance portions of the image. For example, it is possible to emphasize the large-amplitude, small-amplitude, or mid-range signals. It is also possible to perform a more sophisticated analysis to enhance edges.

Many specialty probes have been designed for intracavitary examination. Examples include examination of the fetus with a vaginal probe, the prostate with a rectal probe, and blood vessel walls with intravascular probes. The intracavitary probe offers the advantage of decreasing the distance from the transducer to the tissue of interest and thus decreasing attenuation such that higher frequencies can be used for greater resolution. The lateral resolution of a focused probe is improved with frequency as discussed in the preceding section, but the axial (along the ultrasound beam) resolution also improves with frequency. The shorter the transmitted pulse, the better the axial resolution. Generation of shorter pulses requires sources with a larger bandwidth, which corresponds to a higher center frequency when the sources have bandwidths that are approximately the same fraction of the center frequency.

The use of ultrasound for motion detection and measurement has increased tremendously in recent years. These systems use either the Doppler principle or time-domain detection. In Doppler detection, if the ultrasound is reflected from a target moving at some speed v_t toward (away from) the source at an angle θ with respect to the beam axis, the frequency of the transmitted signal f is shifted up (down) by an amount f_D, the Doppler shift, given by

$$f_D = 2fv_t \cos\theta/c. \tag{4}$$

In principle a measurement of f_D when f, c, and θ are known will yield the speed of the target v_t. However, it is often difficult to determine θ because the angle the transducer axis makes with a blood vessel, for example, is often unknown. Even when that angle is known, the flow is not necessarily along the direction of the vessel at every location and for all times. Time-domain detection of motion, by measuring the movement of specific echoes from one pulse to another, is an alternative to Doppler detection that is used in many ultrasound systems.

For many years duplex systems, which provide both a two-dimensional image and a Doppler signal, showing the change of target speed with time, from a particular selected target area, have been in wide use. More recently color-flow imaging has been employed, which provides a two-dimensional color (typically red or blue) image of flow toward and away from the transducer superimposed on the gray-scale image of stationary tissue structures. For these systems the speed, whether from Doppler or time-domain detection schemes, is indicated by color saturation, hue, or luminance. These systems have proven very valuable for detecting the existence of flow in a region, detecting obstructions to flow and the turbulence associated with this, detecting reduced flow, etc. Some other systems add to the color-flow image a display of speed versus time for a region that is defined by a user-movable box.

1.2 Therapeutic and Other Applications

Though therapeutic applications include the use of vibrating wires to remove plaque and augmentation of liposuction, this article

is concerned with the use of ultrasound for therapeutic heating, hyperthermia, and surgery. These therapeutic applications rely almost exclusively on heating of tissues due to the absorption of the ultrasound. Therapeutic heating involves low temperature elevation in tissues and joints for a period of many minutes for physiotherapy. Typical time-averaged intensities are below approximately 3 W/cm^2. Hyperthermia produces low to moderate temperatures (in the range 43–50 °C) for approximately an hour to treat cancerous tumors, using time-averaged intensities below approximately 10 W/cm^2. In contrast, surgical treatment (sometimes called ablative hyperthermia) uses high-temperature treatment for only a few seconds to destroy tissue immediately. Time-averaged intensities below approximately 1000 W/cm^2 are used to treat the prostate, heart arrhythmia, and tumors in many regions of the body.

The beneficial effects of therapeutic heat have often been cited as increased extensibility of collagen tissues, decreased joint stiffness, pain relief, relief of muscle spasms, assistance in removing inflammatory infiltrates, edema, and exudates, and increased blood flow (Lehmann, 1990).

The rationale for hyperthermic treatment of tumor tissues is based on a belief that tumor tissues (at least some) are more susceptible than normal tissues to damage from elevated temperatures. This has been demonstrated for cells *in vitro* and clinically in patients for many tumor types. Hyperthermic treatment may involve heating the body (whole body hyperthermia), a region of the body that includes the tumor (regional hyperthermia), or the tumor alone (localized hyperthermia). Obviously, localized hyperthermia will have the least impact on normal tissues within the body. Hyperthermia is usually used in conjunction with radiation or chemotherapy. The combined modalities can be much more effective than either alone. For example, radiation has a much reduced effect on hypoxic cells, which are most affected by hyperthermia.

Several other modalities have been used for localized hyperthermia including externally applied microwaves, interstitial microwave antennas, and high-frequency currents. However, microwave frequencies useful for heating with external antennas have a longer wavelength than ultrasound and cannot be as well localized for treating the tumor and avoiding surrounding normal tissues. The use of interstitial microwave antennas involves implantation of many small antennas within the tumor to give a reasonably uniform temperature rise localized to the tumor. The use of high-frequency currents also requires invasive implantation of needle electrodes in arrays that would provide useful heating. On the other hand, bone and air spaces must be avoided with ultrasound, on account of very high attenuation and scattering, respectively. Additionally, "noninvasive" microwave or ultrasound treatment involves the use of invasive thermometry systems to monitor and control the temperature rise in the tumor and surrounding normal tissues.

Therapeutic heating and hyperthermic treatment of surface tumors can be accomplished using unfocused systems. However, since the absorbed power, $P_D = 2\alpha I$ where α is the absorption coefficient, is proportional to intensity I, the treatment depth is dependent upon the frequency because the attenuation coefficient increases with frequency and reduces the intensity much faster with depth. Thus, lower frequencies (on the order of 1 MHz or lower) are used for tumors extending deeper within the body and higher frequencies (on the order of 2–4 MHz) for shallow tumors or tumors with bone located closely behind.

Unfocused systems, which mimic plane-wave exposure, will have the greatest intensity and therefore heating at the body surface. Thus, for the treatment of deep tumors the ultrasound system must provide intensity gain to more than compensate for the attenuation along the path to the tumor so that the time-averaged intensities in the tumor are greater than those in the normal tissues between the body surface and the tumor. Simply stated, this means that the ultrasound entrance window (area) at the body surface must be substantially larger than the cross-sectional area of the tumor. Focusing systems are usually chosen to provide the required gain, but it must be remembered that the focus is scanned over the tumor and that gain in the time-averaged intensities is critical, not simply the static intensity gain of the focusing system.

Another reason that scanned focusing systems are generally used for hyperthermic treatment of deep tumors is so that the spa-

tial power-deposition pattern within the tumor can be controlled to provide a uniform temperature throughout the tumor. Greater deposition at the tumor boundaries will lead to a more uniform temperature because of heat conduction into the tumor interior from the boundaries.

Surgical applications of ultrasound require systems with large intensity gain so that the tissue to be treated can be heated within seconds to a temperature that will destroy the tissue. Then the focal region can be relocated to treat another small volume until the tumor region is entirely destroyed.

Increasingly, systems for hyperthermic treatment of deep tumors and high-intensity focused surgical systems are changing from fixed-focus applicators that are mechanically scanned to electronic, phased-array, focusing systems. These allow rapid scanning without bulky and complex mechanical scanning systems. Additionally, the focal regions of these systems can be modified electronically. For example, the focal region can be made larger so that larger volumes can be affected with each placement of the focus.

In addition to these therapeutic applications of ultrasound, the attenuation and, to a lesser extent, the speed have been used for tissue characterization. This term generally refers to the quantitative measurement of tissue parameters as a means for diagnosis or treatment monitoring. It has been shown, for example, that the measurement of parameters associated with tissue attenuation, such as its magnitude and variation with frequency, can be quite useful to the differentiation between normal and diseased tissues. These applications have proven particularly fruitful in the eye and prostate (Feleppa *et al.*, 1996).

The main thrust of this discussion has been directed toward the medical applications of ultrasound. However, ultrasound biophysics also plays a role in determination of rate constants of chemical reactions through the measure of ultrasonic absorption and speed versus frequency, using horns to generate high intensities for breaking up of biological cells for study of their contents, and to generate cavitation for catalyzing reactions. The biophysical applications of ultrasound are many, and they cannot all be discussed in this article, but it is important to note that most of these applications rely in some way on the direct measurement of, or the knowledge of, the ultrasonic properties of the biological materials. Thus, the next sections of this article directly address the properties of biological materials and techniques for their measurement.

2. ACOUSTICAL CHARACTERISTICS OF BIOLOGICAL MEDIA

The acoustical characteristics of biological media to be discussed here include the loss parameters of attenuation and absorption, the speed of propagation, and the value of the nonlinearity parameter. Though attenuation and absorption are often used interchangeably, they are distinctly different. Absorption refers to the direct conversion of energy to heat as the acoustic wave propagates through the medium. Attenuation, on the other hand, includes absorption and all other processes by which energy is removed or redirected from the ultrasound beam, such as scattering and refraction.

Liquids and biological tissues exhibit a nonlinear relation between the acoustic pressure and the density that is important to the nonlinear propagation associated with high-amplitude waves in the medium. This nonlinear relation can be expressed as a Taylor series expansion with linear, quadratic, and higher-order terms. It has been found that the ratio of the coefficient of the quadratic term to that of the linear term, expressed as the nonlinearity parameter B/A, is very useful to describe nonlinear propagation in the medium.

2.1 Solutions and Suspensions

Solutions and suspensions of biological materials such as amino acids and proteins have been studied extensively in an effort to determine underlying mechanisms of absorption of ultrasound that might be applicable to whole tissues. They offer a simpler biological system for study and, since they are in liquid form, are amenable to measurement by more techniques. For these reasons and others many biological liquids have been measured.

The values for the attenuation and absorption coefficients are the same for solutions and nearly the same for most suspen-

sions. Slight differences might be expected for suspensions of cells or other materials that exhibit an inhomogeneous distribution of density or compressibility that may cause scattering.

In general, all the propagation parameters (attenuation and absorption coefficients, speed, and nonlinearity parameter) increase with the concentration of the molecular species. Thus, it is not sufficient to specify a value for one of these parameters in biological liquids without specifying concentration. Specific values are listed for water, amniotic fluid, and blood in Table 1.

2.2 Tissues

Values for the attenuation coefficient, absorption coefficient, speed, and nonlinearity parameter are listed for water and selected tissues in Table 1. From Table 1 it is clear that bone and lung are very different from most soft tissues within the body. They both exhibit large loss and much higher and lower speeds, respectively. The nonlinearity parameter is generally larger in tissues than water and shows a tendency to increase with structure (Law *et al.*, 1985). On the other hand, the highest value measured for tissues to date is in fat, which also has the lowest speed.

3. MEASUREMENT TECHNIQUES

3.1 Loss Parameters

3.1.1 Attenuation Attenuation measurements may be subdivided into measurements on homogeneous and inhomogeneous media. In homogeneous materials, e.g., liquid solutions, the attenuation is equivalent to the absorption. For inhomogeneous media the attenuation includes absorption, scattering, refraction, etc., any process by which energy is removed from the wave field. While a number of attenuation-measuring techniques also yield absorption for homogeneous materials, there exist perhaps only one or two techniques that measure the absorption coefficient for inhomogeneous materials. The transient thermoelectric technique yields a measure of the absorption coefficient in tissues.

3.1.1.1 Insertion Techniques. This technique may be used with pulsed ultrasound and with phase-sensitive (first-order) or phase-insensitive (second-order) receivers. Continuous-wave (cw) signals may be used when reflection at the interfaces is negligible and when the receiver absorbs or diverts the sound beam so that a standing-wave field is not established (as with a radiation force target). The insertion technique involves the comparison of measurements of the received signal (pulsed or continuous source) with a sample of known thickness between source and receiver and with only the immersion medium between source and receiver; see Fig. 4. If the immersion fluid is of very low attenuation compared to the sample, then its attenuation can be neglected. Let A_0 or B_0 represent the amplitude of the received signal, first- or second-order quantity, respectively, with the sample removed, and let A_s or B_s represent the received signal, first- or second-order quantity, respectively, when a sample of thickness d is placed between the source and receiver. If the reflection at the interfaces is negligible or zero, the attenuation coefficient for the sample material is given by $(20/d)\log(A_0/A_s)$ or $(10/d)\log(B_0/B_s)$ dB/m and by $\ln(A_0/A_s)/d$ or $0.5\ln(B_0/B_s)/d$ Np/m, when d is in meters.

Table 1. Approximate ultrasonic propagation parameters for water and selected tissues at 3.5 MHz. Nonlinearity parameters from Law *et al.* (1985) and other data from Goss *et al.* (1978, 1980).

Tissue	Attenuation coefficient (m^{-1})	Speed (m/s)	Characteristic impedance (10^6 Pa·s/m)	Nonlinearity parameter
Water	0.2	1500	1.50	5.2
Amniotic fluid	0.3	1510	1.51	
Blood	7	1550	1.60	6.5
Fat	25	1470		11
Liver	35	1580	1.74	7.0–7.7
Muscle	50	1560	1.72	
Bone	800	3360	5.70	
Lung	1000	340	0.25	

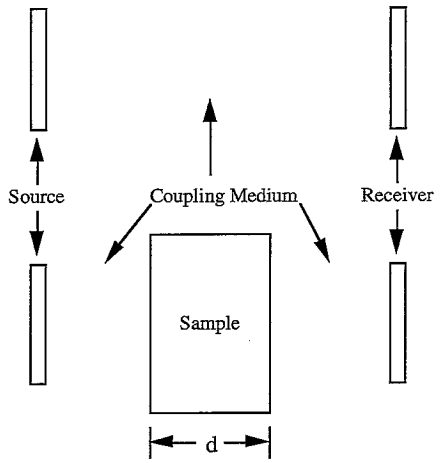

FIG. 4. Schematic representation of the insertion technique. In the upper part of the figure the source and receiver have only a coupling medium between them, whereas in the lower part of the figure a portion of the coupling medium is replaced with a sample of thickness *d*.

The effect of reflection at the interfaces can often be minimized by impedance matching. However, when solids are immersed in liquids the reflections can be very significant. To measure the attenuation coefficient within the sample for such cases, plot the measured attenuation (as opposed to the attenuation coefficient) versus the sample thickness d, as in Fig. 5. The slope gives the attenuation coefficient characteristic of the material, and the intercept ($d = 0$) gives the attenuation due to the interfaces.

The insertion technique has also been used with broad-band transducers and short pulses. Such a system allows spectral analysis of the received signals, with and without the sample present, to determine the attenuation coefficient over a continuous range of frequencies limited by the bandwidth. A spectral-analysis approach has also been used for determination of the attenuation coefficient in fairly homogeneous tissues *in vivo* by measuring the decrease in signal with depth into the tissue (Kuc, 1980). This has been applied most successfully to tissues that can be examined rather directly without having to correct for effects of overlying tissues, such as tissues in the eye and the prostate (Lizzi *et al.*, 1983, 1986).

3.1.1.2 Variable-Path Pulse Techniques. Two measurement methods are described in this section. The first is a method applicable to solids and involves a sample preparation similar to that shown in Fig. 6. Transmitting and receiving transducers are mounted on opposite ends of the solid sample of length d, or a transceiving transducer is placed on one end and the other end left with an air interface to act as a reflector. When the received echos are plotted as a function of distance traveled x (determined from the speed and the length d of the rod), they look like the bold pulses (rectified and filtered rf pulses or video signals) of Fig. 7. The separation between echoes is $2d$. The attenuation coefficient A, neglecting loss at the transducer end, is determined by fitting an exponential curve of the form Be^{-Ax} to the signal levels shown in Fig. 7, where B is the amplitude at $x = 0$.

The same sort of analysis can be performed on a liquid system that has a reflector mounted at a distance d from the transducer. However, it is considerably more difficult to get good parallelism between the transducer and reflector. Therefore, in liquid systems a more common approach [based on

FIG. 5. Straight-line fit to attenuation versus sample thickness. The intercept is loss due to surface reflection, and the slope is the attenuation coefficient of the sample.

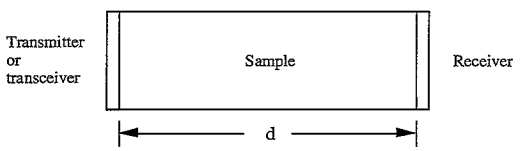

FIG. 6. Schematic diagram of solid sample of length *d* with one (transceiver) or two (transmitter and receiver) transducers mounted on the ends.

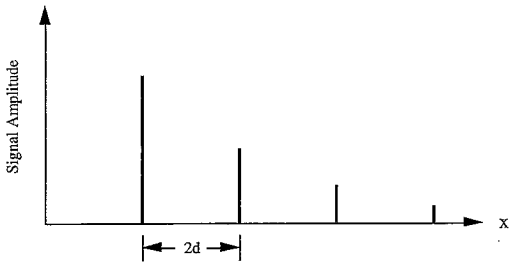

FIG. 7. Signal amplitude versus distance traveled. An exponential fit of the form Be^{-Ax} will yield the attenuation coefficient A, neglecting signal loss at the interfaces and beam diffraction effects.

a technique developed by Pellam and Galt (1946)] is to vary the distance between a source and receiver, smoothly or in discrete steps. These systems may be good over the frequency range from 3 to 100 MHz and higher; however, at the lower frequencies corrections must be made for diffraction effects in the beam.

3.1.1.3 Substitution Method. The effects of diffraction, at low frequencies, are eliminated by using the substitution technique; see Fig. 8. The fixed transducer separation minimizes the effects of diffraction. If the path in the reference medium is z and that in the test liquid is $d - z$, then the received signal A_z is

$$A_z = A_0 \exp(-\alpha_r z) \exp[-\alpha_t(d - z)], \tag{5}$$

where α_r and α_t are the attenuation coefficients in the reference and test liquids, respectively, and A_0 is the signal with no attenuation. When the assembly is moved to a new position such that the path in the reference liquid is $z + \Delta z$, then the received signal $A_{z+\Delta z}$ is

$$A_{z+\Delta z} = A_0 \exp[-\alpha_r(z + \Delta z)] \times \exp[-\alpha_t(d - z - \Delta z)]. \tag{6}$$

Taking the ratio of the two signals, we get

$$A_{z+\Delta z}/A_z = \exp[-(\alpha_r - \alpha_t)\Delta z]. \tag{7}$$

Thus, the slope of the plot of the natural logarithm of the signal ratio versus Δz will give $\alpha_r - \alpha_t$. If α_r is either negligible or known, this gives α_t.

3.1.1.4 Resonant-Cavity System. The resonant-cavity system consists of two transducers separated by a fixed distance that, together with their housing, form a cylindrical cavity in which the test liquid is placed. One transducer serves as a transmitter, while the other is the receiver. When the transmitting transducer is excited with a sinusoidal voltage, standing waves result in the sample and resonances occur at particular frequencies (Eggers, 1968). At the resonance frequencies f_n, the receiving transducer registers pronounced voltage peaks, whose frequency separation depends on the sound speed in the sample, and the half-power (3 dB) bandwidth Δf of which is related to the attenuation per wavelength, $\alpha\lambda$. In fact, the attenuation coefficient of the sample may be calculated from the quality factor Q of the liquid-filled cavity, defined as the resonance frequency f_n divided by the 3 dB bandwidth Δf_n of the resonance. This quality factor is a function of the attenuation per wavelength $\alpha\lambda$ of the ultrasonic energy, and is expressed as

$$Q = (f_n/\Delta f_n) = \pi/\alpha\lambda. \tag{8}$$

The measured Q, however, includes the effect of mechanical clamping of the transducers and losses associated with diffraction, wall effects, imperfect reflections at the transducer surface, etc., besides the desired attenuation due to the liquid. Assuming all of these energy losses are additive (Eggers and Funck, 1973), the measured quality factor Q is given by

$$1/Q_{\text{meas}} = 1/Q_{\text{liquid}} + 1/Q_{\text{extra}}, \tag{9}$$

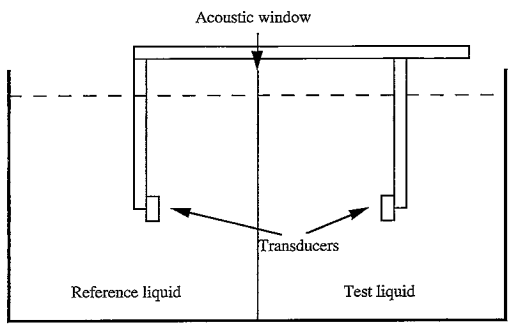

FIG. 8. Schematic diagram of the substitution apparatus.

where Q_{liquid} is the quality factor due to sound absorption in the liquid and Q_{extra} includes all the other cell losses. The absorption can be obtained by means of a reference measurement in the same cell at the same frequencies with a suitable reference liquid, having equal or very similar sound velocity to insure the same sound-field pattern for both measurements. The excess absorption per wavelength in the sample liquid is then obtained from

$$(\alpha\lambda)_{excess} = \pi(\Delta f_s - \Delta f_r)/f_n, \tag{10}$$

where Δf_s and Δf_r are the corresponding 3-dB bandwidths of the nth resonant peak in the sample and reference liquid, respectively.

In general, the transducer separation distance, the character of the ultrasonic field, the cavity shape, and the mechanical and electrical loading of the transducer, in addition to the acoustical properties of the sample liquid, all play significant roles in determining the performance of an ultrasonic resonator. Residual resonator losses such as those due to diffraction, transducer, and wall losses must be minimized so that the quality factor Q is predominantly determined by the sample-liquid absorption. Improvements of Q values for liquid-filled resonators by application of a slight static internal pressure to the cavity have been reported (Eggers and Funck, 1975). The reasons for this improvement seem to be related to the focusing of the sound beam due to the pressure-effected concavity of the transducers, reducing diffraction and side-wall effects, and to the elimination of effects of gaseous inclusions within the cavity.

With the internal pressure these systems have been used to frequencies as low as 0.2 MHz and without the pressure up to 30 MHz and more. These systems present the advantage of requiring only a small volume of sample.

3.1.2 Absorption As stated previously, for homogeneous media with no scatterers present, the absorption and attenuation coefficients are the same, and methods used to measure attenuation can be used to measure absorption. If this is not the case, as with most tissues, the transient thermoelectric technique has been used to measure the absorption coefficient.

The transient thermoelectric technique was developed in 1954 (Fry and Fry, 1954a,b) for measurement of the absorption coefficient in liquids and tissues. This method involves first imbedding a small thermocouple in a tissue sample, then irradiating the combination with an ultrasonic pulse of known intensity. The absorption coefficient α of the imbedding medium is then given as

$$\alpha = \frac{\rho CK}{2I_S}\left(\frac{dT}{dt}\right)_0, \tag{11}$$

where $(dT/dt)_0$ is the initial time rate of change of temperature (°C/s), I_S is the sound intensity at the site of the thermocouple junction (W/cm^2), and ρCK is the product of the surrounding medium's density (g/cm^3) and heat capacity at constant pressure (Cal/g-°C) and the mechanical equivalent of heat (K = 4.186 J/Cal) in units of J/cm$^3\cdot$°C. However, the temperature measured by use of the thermocouple junction is a true measure of the ultrasonic absorption of the surrounding medium only if the ultrasonic beam width is broad enough to minimize the effects of heat conducted away from the junction by the medium, and the size of the thermocouple is reduced to a point where the heat generated by the motion of the viscous medium relative to the thermocouple wire when subjected to ultrasound may be neglected.

The particle motion associated with the sound field causes a relative motion between the wire and the surrounding medium. Because the thermocouples are of small diameter (from a fraction of, to several, thousandths of an inch in diameter), the temperature that results from this relative motion in a viscous medium tends toward an equilibrium value in a short time (fraction of a second). However, the effect is present in a typical measurement of $(dT/dt)_0$; see Fig. 9. The heating from this source is dependent (Fry and Fry, 1954a,b) upon

1. viscosity of the medium,
2. wire size,
3. frequency,
4. the square of the particle velocity, and
5. other physical parameters.

For low-viscosity liquids and tissues, the ef-

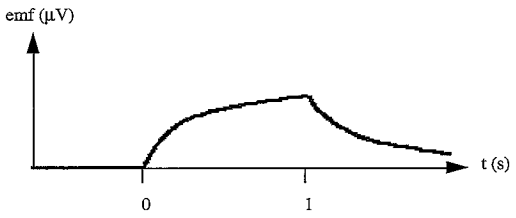

FIG. 9. Typical emf (proportional to temperature) from a thermocouple in an absorbing fluid when exposed to a 1-s ultrasound pulse.

fect of this heat source on the measurement of absorption, when $(dT/dt)_0$ is measured 0.5 s after the sound is initiated, is minimized when the wire diameter is 0.0005 in. (13 μm) or less. For additional information on this effect consult Goss *et al.* (1977).

Since real acoustic beams are not of infinite beam width, heat will diffuse from the position of peak intensity, where the thermocouple junction is located, to the surrounding lower-intensity (cooler) regions, affecting the temperature rise. The effect of this phenomenon on the measured absorption is included by adding a term to Eq. (11) to give

$$\alpha = (\rho CK/2I_S)(dT/dt)_0 + (\kappa/2I_S)\Delta^2 T, \qquad (12)$$

where κ is the thermal conductivity (W/cm-°C). If the rate of heat diffusion, given by $\kappa\Delta^2 T$, is significant, then the α computed from Eq. (11) will be erroneously low. It has been shown (Goss *et al.*, 1977) that the half-power ultrasonic beam width should be at least 3–4 mm to minimize the errors from using Eq. (11) when determining α for most biological tissues.

The intensity at the site of the thermocouple junction I_S should be measured or calculated from the measured intensity with no sample present I_0 from the relation

$$I_S = I_0 e^{-2Ax}, \qquad (13)$$

where A is the pressure attenuation coefficient and x is the path length in the attenuating material, i.e., the thermocouple depth. If the attenuation consists primarily of absorption, then an iterative procedure can be used to calculate α by starting with I_0 instead of I_S. The procedure involves a calculation of α from Eq. (11) with $I_S = I_0$, and the calculation of I_S from Eq. (13) with A equal to this initially calculated α. Then a new calculation of α is performed based on the computed I_S. A new I_S can then be calculated from the new α. This procedure is repeated until the value for α converges (it will converge provided that the product αx is not too large).

3.2 Speed

There exist a variety of speed-measuring techniques that are applicable to liquids and/or solids over specific frequency ranges. The techniques can be separated into pulsed and cw systems. Included in pulse techniques are the time-of-flight, sing-around, variable-path substitution, and pulse superposition methods. The cw systems employ interferometric techniques that involve either a fixed path length and a variable frequency or a fixed frequency and a variable path length. The pulse techniques are applicable to the measurement of both phase and group speeds. Broad-band pulses (short pulses) will yield group speed whereas narrow-band pulses (long pulses containing approximately 10 or 20 cycles or more) will yield the phase speed for the frequency of the rf signal constituting the pulse. Of course, the cw techniques provide phase speed. First the techniques utilizing pulses are discussed.

3.2.1 Time of Flight The straightforward measurement of the time for a pulse to travel through a known length of a specimen is perhaps the simplest means of measuring ultrasonic speed. Figure 6 illustrates the arrangement of source and receiver, or transceiver and reflector, at opposite ends of a solid specimen or a fixed path of liquid as discussed previously. The time of flight or transit time T from source to receiver or the round-trip time $2T$ may be measured by several approaches. The speed c is then given by

$$c = d/T, \qquad (14)$$

where d is the length of the path.

One obvious but low-accuracy approach to determining the transit time is a simple measurement of the delay between transmitted and received pulses by measuring their separation on the time scale of an oscillo-

scope. Oscilloscopes are now generally available with special features that facilitate easy measurement of this time interval via digital readout after adjusting the delayed sweep to superimpose the two echoes. The accuracy of these scopes may be 1% or less, adequate for many simple measurements but rather low compared to some of the very accurate measurement techniques available.

Another means of measuring transit time is to count the number of cycles of a high-frequency timing signal that occur between triggering of the counter by the transmitted pulse and the ending of the count period by the received pulse. The errors in measurement of T for this case will depend upon the frequency of the timing signal and the timing errors of the start and stop control signals. The error arising from the count will be plus or minus one period ΔT of the wave to be counted. Thus for a timing signal of 200 MHz, ΔT will be 5 ns, resulting in a 0.3% error in the velocity of a solid of thickness 1 cm for which the true velocity is 6000 m/s.

Still another method of measuring transit time, the pulse-echo-overlap system, is discussed by Papadakis (1976). In this technique a transceiver system and several echoes from the end of the rod or the reflector are utilized. The echo signals are applied to the vertical axis of an oscilloscope, and a cw signal of variable frequency is applied to the horizontal axis. The principle of measurement is to adjust the frequency of the horizontal-axis signal so that successive echoes overlap. The transit time is then simply the period of this signal, which can be determined by an accurate measurement of frequency.

3.2.2 Sing-Around Method A block diagram of a sing-around system for velocity measurement is illustrated in Fig. 10. The principle of operation in this system is that the received pulse triggers another pulse so that a repetitive trigger signal occurs at a rate equal to the reciprocal of the propagation time. The frequency and thus the period between trigger pulses can be very accurately measured and the system is easily automated. However, any timing delays associated with the electronics will show up as errors in the determination of transit time. These electrical delays may be minimized by appropriate signal processing. This system is

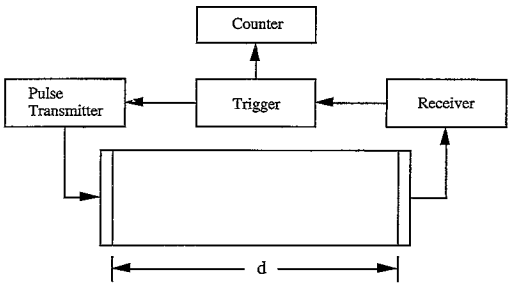

FIG. 10. Block diagram of the sing-around system for velocity measurement.

easily good to 1% (this is dependent upon path length) for absolute measurements but is several orders of magnitude more accurate when used as a comparison technique.

3.2.3 Variable-Path Method Another pulse method involves two transducers (a source and a receiver) whose separation is changed, e.g., increased at a constant rate by a motor and drive screw. Since the separation between transducers is continuously varied, these systems are restricted to measurements in liquids. Speed measurements are accomplished by algebraically adding a continuous-wave reference signal to the output of the receiver. The addition produces an interference pattern that exhibits a peak or minimum (a null if both signals are of equal amplitude) when the two signals are in or out of phase, respectively. The maxima occur every half wavelength, so that the velocity is easily determined after measuring the distance between maxima. These systems are used for measurements at higher frequencies where diffraction effects are smaller, e.g., over the frequency range from a few megahertz to 100 MHz.

3.2.4 Substitution Method The substitution or velocity-difference method is similar to the moving-transducer method in that the pulses are transmitted from a source to a receiver and the received signal is electronically mixed with a continuous-wave reference. However, in this method the two transducers are maintained at a fixed distance from each other, the changing phase of the received signal arising from substitution of the test liquid for a reference liquid over a portion of the signal path (Carstensen, 1954); see Fig. 8. One transducer is placed in the

test liquid and the other in the reference liquid, which is separated from the test liquid by an acoustically transparent window. The substitution of one liquid for another is effected by moving the two-transducer assembly via micrometer or motor control.

The fixed transducer separation provides to this technique a way of virtually eliminating the effects of diffraction on the measurements of speed and attenuation. Thus it finds application in the low-frequency range, 0.3–15 MHz, where the errors incurred with the moving-transducer technique are unacceptably large. The accuracy of this method is good to 1 part in 10^4, provided adequate temperature control (± 0.1 °C) is maintained and the speed in the reference medium is known to that accuracy. This technique has proven useful to the investigation of dispersion in biological liquids (may be less than 0.1%). Typically, water, which is dispersionless in this frequency range, is used as the reference liquid.

To examine the technique in more detail, consider z to be the initial path length in the reference medium (taken as water in this example) and d to be the transducer separation. The number of acoustic wavelengths separating the transducers n is given by

$$n = z/\lambda_R + (d - z)/\lambda_X, \tag{15}$$

where λ_R is the wavelength in the reference medium and λ_X is the wavelength in the test liquid. If the transducer assembly is moved a distance Δz to go from one minimum in the received signal to another, the new relation for the number of wavelengths becomes, for $\lambda_X > \lambda_R$,

$$n + 1 = (z + \Delta z)/\lambda_R + (d - z - \Delta z)/\lambda_X. \tag{16}$$

This may be rearranged to give

$$c_X - c_R = c_R^2[1/(f\Delta z - c_R)], \tag{17}$$

where f is the frequency and c_R and c_X are the speeds in the reference and test liquid, respectively.

3.2.5 Continuous-Wave Techniques Continuous-wave techniques measure the variation in transducer parameters such as input impedance, voltage, or current in a standing-wave field as the transducer position or frequency is changed. Let us examine the specific acoustic impedance at the surface of a transducer located a distance L from a reflector; see Fig. 11. The acoustic pressure p_I of the wave incident on the reflector, the pressure p_R of the reflected wave, and their respective particle velocities u_I and u_R are given as follows:

$$\begin{aligned} p_I &= P_I e^{j(\omega t - kx)}, \\ p_R &= rP_I e^{j(\omega t + kx)}, \\ u_I &= (P_I/Z)e^{j(\omega t - kx)}, \\ u_R &= -(rP_I/Z)e^{j(\omega t + kx)}, \end{aligned} \tag{18}$$

where r is the complex reflection coefficient, Z is the characteristic impedance of the material, and the reflector is located at $x = 0$.

The specific acoustic impedance at a transducer located at position L will vary from infinity at a perfectly reflecting surface through zero at one-quarter wavelength from the reflector, back to infinity at one-half wavelength from the reflector, etc. Maxima in the impedance are spaced one-half wavelength apart, as are minima. Thus, the spacing for impedance maxima, or minima, can be measured to yield the speed.

3.2.6 Pulse-Superposition Method In some respects the pulse-superposition method is similar to the pulse-echo overlap technique. By superimposing the input signals over the echoes from the end of a rod of the material, the period T_0 between successive rf pulses can be measured and is given by

$$T_0 = hD - h\nu/2\rho f + n/f, \tag{19}$$

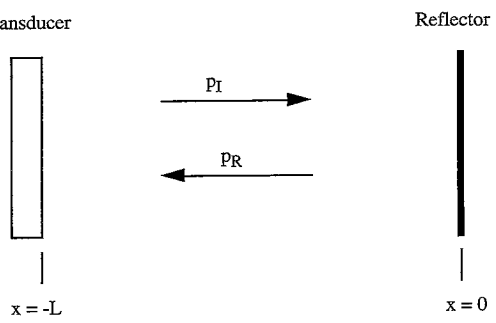

FIG. 11. A transducer and a reflector producing a standing-wave field.

where D is the round-trip delay time in the material (the parameter of interest), h is the number of round-trips through the material, v is the phase angle associated with reflection at the transducer end, n is the number of wavelengths by which pulses are shifted with respect to one another, and f is the frequency of the ultrasound pulse. The value of h is known as a part of the measurement technique, and values for v and n can be determined as described by McSkimin (1964). Thus D and the speed in a rod of known length can be determined. Consult McSkimin (1964) for more details of the technique.

A pulse-superposition technique can also be used to determine the specific acoustic impedance of shear waves in liquids. The complex reflection coefficient is determined for shear waves at the interface between a solid buffer rod of known impedance and the liquid. This is done by measuring the change in the period between successive pulses in the buffer rod (and amplitude of the pulses) when the rod termination is changed from air (perfect reflection) to the liquid to be measured.

The schematic of one system that can be used to accomplish the measurement is illustrated in Fig. 12. The repetition rate of a rf pulse generator is accurately controlled and measured. The pulse-train signal is split and each signal passed through a gate. The signal passed by gate B is attenuated before the two signals are recombined and applied to a shear transducer bonded to the buffer rod. The multiple echoes are received and displayed.

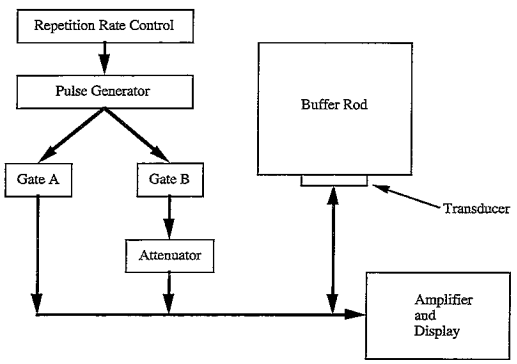

FIG. 12. Block diagram of a simple pulse-superposition system.

Figure 13 demonstrates the application of the technique. With an air interface at the end of the rod, the two gates [Fig. 13(b)] can be adjusted to let two rf pulses from the pulse train [Fig. 13(a), sinusoidal rf signal in pulses not shown], separated in time so that their echos do not overlap [Fig. 13(c)], pass to the transducer. The first echo of the B pulse is attenuated to equal the magnitude of a chosen echo of the A pulse. In Fig. 13(c) the video signals are illustrated wherein the third echo of the A pulse has been matched in amplitude by the first echo of the B pulse, $h = 2$ for this case. Then the B gate is adjusted to let an earlier pulse through so that

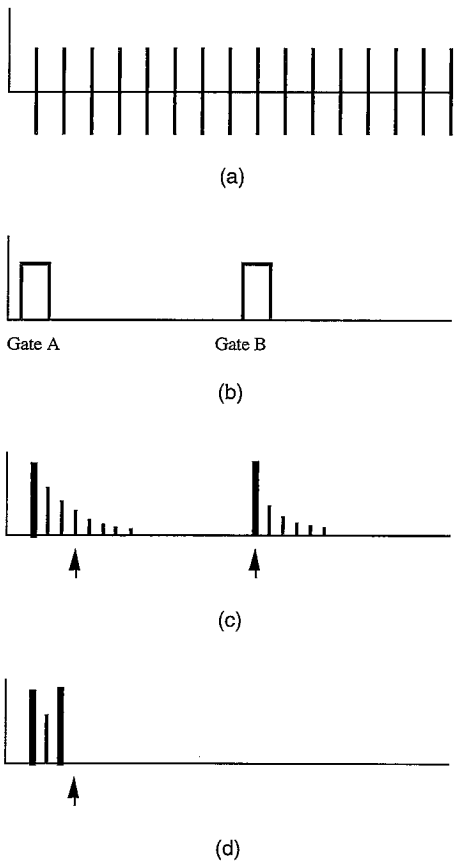

FIG. 13. Illustration of signals when using the superposition technique. (a) Selected rf signals are passed by (b) gates A and B. (c) In this example, the first echo from the gate-B series is matched in amplitude to the third echo from the gate-A series. (d) Gate B is moved and the pulse repetition frequency is adjusted to cancel echo 3 and higher from the gate-A series.

the two echoes mentioned are superimposed. The pulse repetition rate is finely adjusted to cancel the third and succeeding echos of the A pulse, Fig. 13(d). At this point the period T_0 between pulses A_3 and B_1 is given by Eq. (19) where $h = 2$. Then the liquid sample is placed on the end of the buffer rod and the same procedure followed to yield a new period:

$$T = hD - h(v - \epsilon)/2\pi f + n/f, \tag{20}$$

where ϵ is the phase angle associated with reflection from the interface with the liquid. If T_0 and T are expressed in terms of the repetition rate frequencies $f_R = 1/T$ and $f_{R0} = 1/T_0$ and Eqs. (19) and (20) are combined, the following expression for ϵ is obtained:

$$\epsilon = 2\pi f(f_{R0} - f_R)/hf_R f_{R0}. \tag{21}$$

The magnitude of the reflection coefficient is determined by measuring the change in magnitude of A_4 (the change in attenuation, ΔM) that occurs upon application of the sample to the buffer rod. This is related to the magnitude of the reflection coefficient as

$$\Delta M = hB = -20h \log P, \tag{22}$$

where ΔM is the change in the magnitude of the echo of interest in decibels, B is the change in the magnitude in decibels per impingement (echo), and P is the magnitude of the reflection coefficient (assuming total reflection from the buffer rod–air interface). This technique has proven useful in the 2–40-MHz frequency range for a number of liquids of interest (Dyro, 1972) and in tissues (Frizzell *et al.*, 1976).

3.3 Nonlinearity Parameter

The following is a brief summary of some of the techniques that have been used to measure the nonlinearity parameter B/A for biological materials. The thermodynamic method requires the accurate measure of the change in speed that occurs, either under adiabatic conditions or separately as a function of temperature and pressure; see Figs. 14 and 15. In the former approach, the speed is measured before and immediately after a rapid change in pressure, before significant heat flow can occur (change in speed measured at approximately 1 s in Fig. 15). The change in speed is determined from a measure of the change in phase of the received signal as illustrated in Fig. 14. Measurements of this type have been recently reported by Sehgal and Greenleaf (1984). From a knowledge of the change in speed with change in pressure at constant entropy, ρ_0, and c_0, B/A can be determined using the following relation:

$$\frac{B}{A} = 2\rho_0 c_0 \left(\frac{\partial c}{\partial p}\right)_{S,\rho=\rho_0}. \tag{23}$$

It can also be shown that the expression above for B/A is equivalent to

$$\frac{B}{A} = 2\rho_0 c_0 \left(\frac{\partial c}{\partial p}\right)_{T,\rho_0} + \frac{2\beta_V T c_0}{C_P}\left(\frac{\partial c}{\partial T}\right)_{p,\rho_0}, \tag{24}$$

where $\beta_V = V^{-1}(\partial V/\partial T)_P$ is the volume coef-

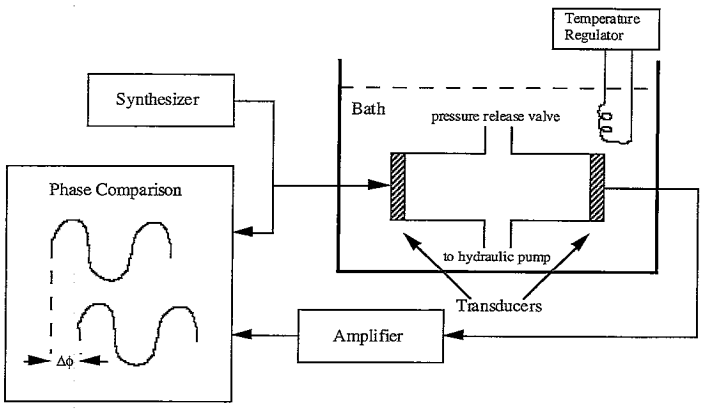

FIG. 14. Block diagram of system used to measure B/A by making speed measurements during a pressure change at constant entropy.

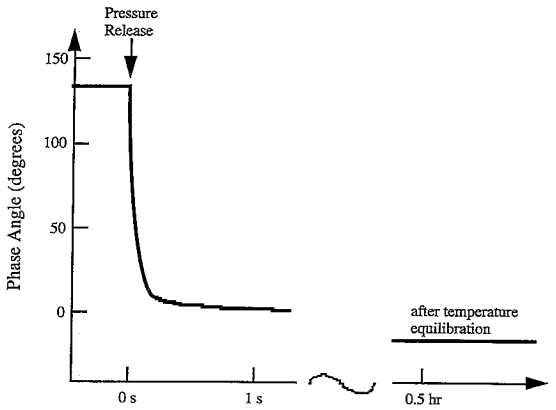

FIG. 15. Change in phase of received waveform (wave speed) with time after rapid pressure change. Final value after temperature equilibration.

ficient of thermal expansion, V is the volume, P is the pressure, C_p is the specific heat at constant pressure, and T is the temperature. Thus measurements of the speed as a function of temperature at constant pressure and as a function of pressure at constant temperature (measurement of change after approximately 0.5 h in Fig. 15) will give the two partial derivatives above. These and the values for β_v and C_p will allow computation of B/A. An example of a system that can be used to make such measurements was described by Law *et al.* (1985). This technique is also potentially very accurate but requires much longer measurement time for appropriate temperature equilibration.

Another class of measurement techniques has been referred to as finite-amplitude methods. These techniques employ the measurement of a harmonic component or components of the wave versus distance from the source. For example, for an ideal plane wave in a lossless material the Fubini solution to the nonlinear wave equation, describing the development of harmonics close to the source, gives the following rather simple form:

$$p_n(\sigma) = [2p_1(0)/n\sigma]J_n(n\sigma), \tag{25}$$

where $p_1(0)$ is the amplitude of the fundamental at the source, J_n is the nth-order Bessel function, and $\sigma = x/L$ where x is the distance from the source and L is the discontinuity distance (distance at which a shock wave starts to develop) (Beyer, 1974). Examining $n = 2$, i.e., the second-harmonic component, yields

$$\frac{B}{A} = \frac{2\rho_0 c_0^3}{\pi f}\frac{p_2(x)}{xp_1(0)^2} - 2, \tag{26}$$

where $p_2(x)$ is the value of the second harmonic as a function of distance from the source, x. This can be experimentally measured by using a receiver that is sensitive to the second harmonic and by varying the distance between source and receiver; see Fig. 16.

This is a valid determination of B/A if we take the intercept for $p_2(x)/xp_1(0)^2$. Thus

$$\frac{B}{A} = \frac{2\rho_0 c_0^3}{\pi f}\left[\frac{p_2(x)}{xp_1(0)^2}\right]_{xp_1(0)\to 0} - 2. \tag{27}$$

In lossless materials this bracketed function would be a horizontal line, but in lossy media it will intercept at an angle. However, it will be a straight line on a semilog plot (Fig. 17) such that the intercept is still valid (and easily obtained) for the determination of B/A. More details of this measurement approach can be found elsewhere (Law *et al.*, 1985). This technique is less accurate than the thermodynamic approach, but it does allow *in vivo* measurements that are not possible using thermodynamic systems, which require pressurization.

There are other acoustical methods used for measuring B/A that utilize "pump" and "probe" waves (Cain, 1986). The high-amplitude "pump" wave provides the pressure change for the low-amplitude "probe" wave. Such approaches present the possibility of imaging B/A; however, the details are quite complicated and one cannot directly measure B/A.

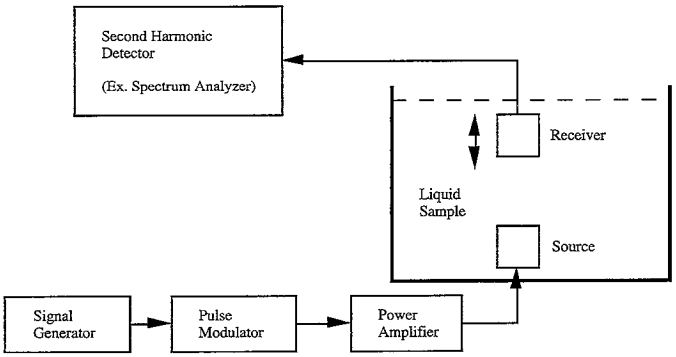

FIG. 16. Block diagram of system for measuring p_2 versus x.

4. RECENT ADVANCES IN MEDICAL IMAGING AND THERAPY

As mentioned previously, phased arrays have seen increasing use in both medical imaging and therapy. Linear arrays for medical imaging have become the norm for producing two-dimensional clinical images. However, ideally a full two-dimensional array would be used to generate a focus that could be scanned in three dimensions. The problem is that to eliminate grating lobes by keeping the interelement spacing on the order of one-half the wavelength leads to a very large number of elements that makes fabrication of fully filled transducers and the associated electronics too complex and costly. Thus, linear arrays, which allow focusing and movement of the focus in one plane, have been used almost exclusively.

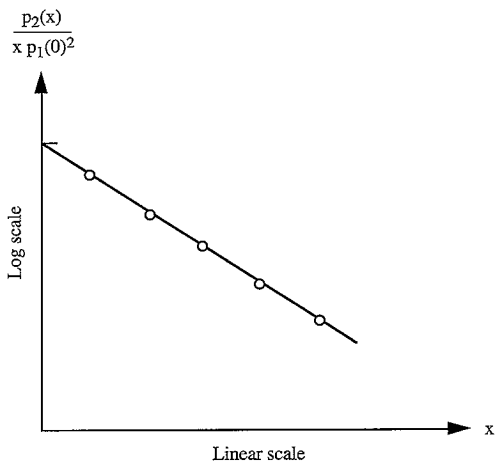

FIG. 17. Plot of parameter to determine B/A.

The thickness of this two-dimensional "slice" has been typically controlled by weak focusing in the other dimension using a cylindrical lens or a curved source.

Recently the slice thickness has been decreased by the use of 1.5-D arrays. These are similar to the linear arrays except that they also have a few elements, to date typically no more than 5 or 7, in the other direction. Though these are not true two-dimensional arrays, they do allow the use of phasing to modify the slice thickness from what it would be with the standard mechanical focusing alone. These arrays are used increasingly in imaging systems.

Another advancement is three-dimensional imaging, the acquisition of signals from a three-dimensional volume of tissue (Tong *et al.*, 1996). This is accomplished by the systematic acquisition of two-dimensional images. The data from these can then be used, via specialized algorithms, to view two-dimensional images in various planes of choice and to determine volumes of organs, chambers, etc. much more accurately (Gilja *et al.*, 1995). Currently, three-dimensional image data are not viewed in real time, but only after some off-line processing time. However, the processing time is steadily decreasing, and these systems will be very useful in future ultrasound medical imaging.

Therapeutic ultrasound developments also center very much around the use of phased arrays for electronic control of treatment (Chapelon *et al.*, 1993; Fan and Hynynen, 1994; Wan *et al.*, 1995; Kluiwstra *et al.*, 1995; Hutchinson *et al.*, 1995; Goss *et al.*, 1996). Different groups have taken different approaches to the development of systems that employ phased-array technology but with a

limited number of elements. Phased-array systems have been proposed for treatment of the heart (Kluiwstra *et al.,* 1995), the prostate (Hutchinson *et al.,* 1995), and other regions of the body (Wan *et al.,* 1995; Goss *et al.,* 1996).

Works Cited

AIUM (1993), *Bioeffects and Safety of Diagnostic Ultrasound,* Laurel, MD: American Institute of Ultrasound in Medicine, p. 86.

Cain, C. A. (1986), *J. Acoust. Soc. Am.* **80,** 28–32.

Carstensen, E. L. (1954), *J. Acoust. Soc. Am.* **26,** 858–861.

Chapelon, J. Y., Faure, P., Plantier, M., Cathignol, D., Souchon, R., Gorry, F., Gelet, A. (1993), in: M. Levy, B. R. McAvoy (Eds.), *Proceedings of the 1993 IEEE Ultrasonics Symposium,* Piscataway, NJ: IEEE, pp. 1211–1214.

Dyro, J. F. (1972), Ph.D. Thesis, University of Pennsylvania, Philadelphia.

Eggers, F. (1968), *Acustica* **19,** 323–328.

Eggers, F., Funck, Th. (1973), *Rev. Sci. Instrum.* **44,** 969–977.

Eggers, F., Funck, Th. (1975), *J. Acoust. Soc. Am.* **57,** 331–333.

Fan, X., Hynynen, K. (1994), *Med. Phys.* **22,** 297–306.

Feleppa, E. J., Kalisz, A., Sokil-melgar, J. B., Lizzi, F. L., Liu, T., Rosando, L., Shao, M. C., Fair, W. R., Wang, Y., Cookson, M. S., Reuter, V. E., Heston, W. D. W. (1996), *IEEE Trans. Ultrason. Ferroelec. Freq. Control* **UFFC-43,** 609–619.

Frizzell, L. A., Carstensen, E. L., Dyro, J. F. (1976), *J. Acoust. Soc. Am.* **60,** 1409–1411.

Fry, W. J., Fry, R. B. (1954a), *J. Acoust. Soc. Am.* **26,** 294–310.

Fry, W. J., Fry, R. B. (1954b), *J. Acoust. Soc. Am.* **26,** 311–317.

Gilja, O. H., Smievoll, A. I., Thune, N., Matre, K., Hausken, T., Odegaard, S., Berstad, A. (1995), *Ultrasound Med. Biol.* **21,** 25–32.

Goss, S. A., Cobb, J. W., Frizzell, L. A. (1977), in: J. deKlerk, B. R. McAvoy (Eds.), *1977 Ultrasonics Symposium Proceedings,* Piscataway, NJ: IEEE, pp. 206–211.

Goss, S. A., Johnston, R. L., Dunn, F. (1978), *J. Acoust. Soc. Am.* **64,** 423–457.

Goss, S. A., Johnston, R. L., Dunn, F. (1980), *J. Acoust. Soc. Am.* **68,** 93–108.

Goss, S. A., Frizzell, L. A., Kouzmanoff, J. T., Barich, J. M., Yang, J. M. (1996), *IEEE Trans. Ultrason. Ferroelec. Freq. Control* **UFFC-43,** 1111–1121.

Haney, M. J., O'Brien, Jr., W. D. (1986), in: J. F. Greenleaf (Ed.), *Tissue Characterization with Ultrasound,* Vol. 1, Boca Raton, FL: CRC Press, Chap. 2.

Hutchinson, E. B., Buchanan, M. T., Hynynen, K. (1995), in: M. Levy, S. C. Schneider, B. R. McAvoy (Eds.), *Proceedings of the 1995 IEEE Ultrasonics Symposium,* Piscataway, NJ: IEEE, pp. 1601–1604.

Kino, G. S. (1987), *Acoustics: Devices, Imaging, and Analog Signal Processing,* Englewood Cliffs, NJ: Prentice-Hall.

Kinsler, L. E., Frey, A. R., Coppens, A. B., Sanders, J. V. (1982), *Fundamentals of Acoustics,* 3rd ed., New York: Wiley.

Kluiwstra, J.-U., Zhang, Y., VanBaren, P., Strickberger, S. A., Ebbini, E. S., Cain, C. A. (1995), in: M. Levy, S. C. Schneider, B. R. McAvoy (Eds.), *Proceedings of the 1995 IEEE Ultrasonics Symposium,* Piscataway, NJ: IEEE, pp. 1605–1608.

Kuc, R. (1985), *Proc. IEEE* **73,** 1159–1163.

Law, W. K., Frizzell L. A., Dunn, F. (1985), *Ultrasound Med. Biol.* **11,** 307–318.

Lehmann, J. F., de Lateur, B. J. (1990), in: J. F. Lehmann (Ed.), *Therapeutic Heat and Cold,* 4th ed., Baltimore: Williams and Wilkins, Chap. 9.

Lizzi, F. L., Greenebaum, M., Feleppa, E. J., Elbaum, M., Coleman, D. J. (1983), *J. Acoust. Soc. Am.* **73,** 1366–1373.

Lizzi, F. L., Ostromogilsky, M., Feleppa, E. J., Rorke, M. C., Yaremko, M. M. (1986), *IEEE Trans. Ultrason. Ferroelec. Freq. Control* **UFFC-33,** 319–329.

McSkimin, H. J. (1964), in: W. P. Mason (Ed.), *Physical Acoustics,* Vol. I, New York: Academic, Chap. 4.

Papadakis, E. P. (1976), in: W. P. Mason and R. N. Thurston (Eds.), *Physical Acoustics,* Vol. XI, New York: Academic, Chap. 5.

Pellam, J. R., Galt, J. K. (1946), *J. Chem. Phys.* **14,** 608–614.

Sehgal, C. M., Greenleaf, J. F. (1984), *J. Acoust. Soc. Am.* **76,** 1023–1029.

Suslick, K. (Ed.) (1988), *Ultrasound: Chemical, Physical, and Biological Effects,* New York: VCH Publishers.

Tong, S., Downey, D. B., Cardinal, H. N., Fenster, A. (1996), *Ultrasound Med. Biol.* **22,** 735–746.

Wan, H., VanBaren, P., Ebbini, E., Cain, C. (1995), in: M. Levy, S. C. Schneider, B. R. McAvoy (Eds.), *Proceedings of the 1995 IEEE Ultrasonics Symposium,* Piscataway, NJ: IEEE, pp. 1623–1628.

Further Reading

Beyer, R. T. (1974), *Nonlinear Acoustics,* Washington, DC: Naval Ship Systems Command, Department of the Navy.

Breazeale, M. A., Cantrell, J. H., Jr., Heyman, J. S. (1981), in: P. D. Edmonds (Ed.), *Methods of Experimental Physics: Ultrasonics,* Vol. 19, New York: Academic, Chap. 2.

Christensen, D. A. (1988), *Ultrasonic Bioinstrumentation,* New York: IOP Publishing.

Fullerton, G. D., Zagzebski, J. A. (Eds.) (1980), *Medical Physics of CT and Ultrasound,* New York: American Institute of Physics.

Hill, C. R. (1986), *Physical Principles of Medical Ultrasonics,* New York: Wiley.

Kremkau, F. W. (1993), *Diagnostic Sonography: Principles and Instruments,* 4th ed., Philadelphia: W. B. Saunders Co.

Tsui, B., Smith, M., Shung, K. K. (1992), *Principles of Medical Imaging,* New York: Academic.

Webb, S. (Ed.) (1988), *The Physics of Medical Imaging,* New York: IOP Publishing.

Wells, P. N. T. (1977), *Biomedical Ultrasonics,* New York: Academic.

Wells, P. N. T., Ziskin, M. C. (Eds.) (1980), *New Techniques and Instrumentation in Ultrasonography,* New York: Churchill Livingstone.